

Study on the composition profile of a $\text{Hg}_{1-x}\text{Cd}_x\text{Te}$ epitaxy film by infrared transmission spectroscopy

This article has been downloaded from IOPscience. Please scroll down to see the full text article.

1995 J. Phys.: Condens. Matter 7 29

(<http://iopscience.iop.org/0953-8984/7/1/004>)

View [the table of contents for this issue](#), or go to the [journal homepage](#) for more

Download details:

IP Address: 171.66.16.179

The article was downloaded on 13/05/2010 at 11:37

Please note that [terms and conditions apply](#).

Study on the composition profile of a $\text{Hg}_{1-x}\text{Cd}_x\text{Te}$ epitaxy film by infrared transmission spectroscopy

Biao Li, Junhao Chu, Kun Liu and Dingyuan Tang

National Laboratory for Infrared Physics, Shanghai Institute of Technical Physics, Academia Sinica, 320 Zhong Shan Bei Yi Road, Shanghai 200083, People's Republic of China

Received 31 January 1994, in final form 29 September 1994

Abstract. Based on our empirical rules for the intrinsic absorption coefficient and refractive index of $\text{Hg}_{1-x}\text{Cd}_x\text{Te}$ in Hougen's model, a useful method for determining the composition profile of an epitaxy layer from room-temperature infrared transmittance spectroscopy is presented. The compositional depth non-uniformity of $\text{Hg}_{1-x}\text{Cd}_x\text{Te}$ film samples grown by liquid-phase epitaxy, metal-organic chemical vapour deposition and molecular beam epitaxy techniques is determined using this method and compared with that from secondary ion mass spectroscopy and x-ray microprobe measurements.

1. Introduction

Recently, considerable interest has developed in the growth of $\text{Hg}_{1-x}\text{Cd}_x\text{Te}$ thin films for the requirements of fabrication and production of advanced infrared images and focal plane arrays. It is well known that $\text{Hg}_{1-x}\text{Cd}_x\text{Te}$ epitaxy films always have a graded composition profile which has a great influence on the performance of a device [1]; so it is important to find an effective method of identifying its composition distribution and to ascertain its suitability for making a device. Although secondary-ion mass spectroscopy (SIMS) [2], energy-dispersive x-ray analysis (EDXA) (with a cleaved sample) and x-ray microprobe measurements (with a taped-etched sample) can be used to derive the composition profile well, they are all destructive methods [3]. Hence infrared transmittance spectroscopy is an attractive technique for characterizing $\text{Hg}_{1-x}\text{Cd}_x\text{Te}$ material because it is a convenient non-destructive method [3–7]. The transverse compositional non-uniformity of bulk $\text{Hg}_{1-x}\text{Cd}_x\text{Te}$ has been determined from the measured transmittance curve in a large test area of the samples at room temperature [5]. Furthermore, Hougen [6] has put forward a model for infrared absorption and transmittance of liquid-phase epitaxy (LPE) $\text{Hg}_{1-x}\text{Cd}_x\text{Te}$, and we have obtained empirical rules for the intrinsic absorption coefficient [8, 9] and refractive index [10] of $\text{Hg}_{1-x}\text{Cd}_x\text{Te}$. Based on these, the composition depth non-uniformity of an epitaxy layer can be determined from the room-temperature infrared transmission for different $\text{Hg}_{1-x}\text{Cd}_x\text{Te}$ films grown by LPE, metal-organic chemical vapour deposition (MOCVD) and molecular beam epitaxy (MBE). The composition profiles obtained by this method agree well with those from SIMS measurement.

2. Calculation of infrared transmission

In his model, Hougen has considered the multiple reflections between three interfaces: air to epilayer (subscript 1), epilayer to transparent substrate (subscript 2) and substrate to air

(subscript 3). He deduced the transmission for light passing through the $\text{Hg}_{1-x}\text{Cd}_x\text{Te}$ film to be

$$T_{1,3} = (1 - R_1)(1 - H)T_{2,3}a_1/[1 - R_1(1 - H)R_{2,3}a_1^2] \quad (1)$$

where

$$T_{2,3} = (1 - R_2)(1 - R_3)a_2/[1 - R_2R_3a_2^2] \quad (1a)$$

$$R_{2,3} = R_2 + R_3(1 - R_2)^2a_2^2/[1 - R_2R_3a_2^2] \quad (1b)$$

$$a_2 = \exp(-\alpha_{mct}t_{mct}) \quad (1c)$$

$$a_2 = \exp(-\alpha_s t_s). \quad (1d)$$

The parameter H represents the fraction of light lost at the epilayer surface and is treated as a variable parameter to match the maximum measured transmission to the calculated transmission. R_1 , R_2 , R_3 and R_4 are the reflectivities at the four interfaces, respectively, and can be obtained from

$$R = (n_i - n_j)^2/(n_i + n_j)^2. \quad (2)$$

The refractive index n is related to the wavelength λ , Cd concentration x and temperature T . Here we need the refractive index near the band-gap energy. The empirical formula has been derived recently from intrinsic absorption spectroscopy using Kramers-Kronig (KK) calculation [10] as

$$n(\lambda, T, x)^2 = A + B/[1 - C/\lambda^2] + D\lambda^2 \quad (3)$$

where

$$A = 13.173 - 9.582x + 2.909x^2 + 10^{-3}(300 - T) \quad (3a)$$

$$B = 0.83 - 0.246x - 0.0961x^2 + 8 \times 10^{-4}(300 - T) \quad (3b)$$

$$C = 6.706 - 14.437x + 8.531x^2 + (0.612 - 2.777x + 3.252x^2)(300 - T) \quad (3c)$$

$$D = 1.953 \times 10^{-4} - 0.00128x + 1.853 \times 10^{-4}x^2. \quad (3d)$$

The absorption term, as a function of frequency, for the epilayer is

$$\alpha(k, T)d = \int \alpha[k, T, x, (z)] dz \quad (4)$$

where d , T and K are the thickness of the epilayer, the temperature and the wavenumber, respectively. The complete intrinsic absorption of $\text{Hg}_{1-x}\text{Cd}_x\text{Te}$ includes the Urbach exponential-absorption edge and intrinsic absorption in the Kane region. The Urbach absorption edge can be expressed by the empirical equation [8]

$$\alpha = \alpha_0 \exp[\alpha(E - E_0)/k_B T] \quad (5)$$

where

$$\ln \alpha_0 = -18.5 + 45.68x \quad (5a)$$

$$E_0 = -0.355 + 1.77x \quad (5b)$$

$$\sigma/kT = (\ln \alpha_g - \ln \alpha_0)/(E_g - E_0) \quad (5c)$$

$$\alpha_g = -65 + 1.88T + (8694 - 10.31T)x \quad (5d)$$

$$E_g = -0.295 + 1.87x - 0.28x^2 + (6 - 14x + 3x^2)(10^{-4}T) + 0.35x^4 \quad (5e)$$

While the intrinsic absorption in the Kane region can be described as [9]

$$\alpha = \alpha_g \exp[\beta(E - E_g)]^{1/2} \quad (6)$$

where

$$\beta = -1 + 0.083T + (21 - 0.13T)x \quad (6a)$$

On the assumption that the transverse composition of the $\text{Hg}_{1-x}\text{Cd}_x\text{Te}$ epilayer is constant, then the composition depth profile of the $\text{Hg}_{1-x}\text{Cd}_x\text{Te}$ film can be written [6]

$$x(z) = [1 - (x_s + sd)]/[1 + 4(z/dz)^2] + (x_s + sd) - sz \quad (7)$$

where d is the thickness of the epilayer, z is the distance from the substrate, and x_s , s and dz are fitting parameters. When equations (2)–(7) are substituted into equation (1), the transmission of the $\text{Hg}_{1-x}\text{Cd}_x\text{Te}$ sample can be calculated. The parameters x_s , s and dz in equation (7) are adjusted to match equation (1) to the measured room-temperature transmission. These three parameters are not totally independent; primarily, s is related to the cut-off slope, x_s to the Cd concentration at the film surface, s to the slope of compositional grading, and dz to the width of CdTe diffusion at the substrate-epilayer interface.

In some cases, the theoretical transmission curve derived from equations (1)–(7) cannot match the experimental data very well, irrespective of how the parameters s , x_s and dz are adjusted in equation (7). This is due to the transverse composition non-uniformity of the $\text{Hg}_{1-x}\text{Cd}_x\text{Te}$ sample [5, 7, 11] which is not included in Hougen's model in equation (7). To make the theory agree better with experiment, one should consider the actual composition distribution, i.e. the composition non-uniformities in both the longitudinal (the depth profile) and the transverse direction. According to equation (1) in [5], the whole spatial composition profile of the $\text{Hg}_{1-x}\text{Cd}_x\text{Te}$ epilayer is assumed to obey the normal distribution

$$f(x) = \exp\{-[x(z) - x]^2/2\sigma^2\}/(2\pi)^{1/2}\sigma x(z) \quad (8)$$

where $f(x)$ is the probability of an x -value in the epilayer plane at a distance of z from the interface. x refers to the real Cd concentration and σ to the concentration deviation in the plane. This indicates that the concentration is distributed between $x(z) - 2\sigma$ and $x(z) + 2\sigma$ with a probability of about 95.44%. Hence equation (8) may be more appropriate for describing the practical composition profile.

3. Experiment results and discussion

The $\text{Hg}_{1-x}\text{Cd}_x\text{Te}$ samples were grown by the LPE, MOCVD and MBE techniques, with epilayer thicknesses ranging from 6 to 30 μm . The substrates for LPE growth were CdTe. In the MBE and MOCVD cases, the substrates were GaAs; a CdTe buffer layer was grown first followed by a narrow-gap $\text{Hg}_{1-x}\text{Cd}_x\text{Te}$ film. With a view to understanding the composition depth profile of the epilayer better, the sample should be selected so that its transverse composition is constant. A convenient method for determining the transverse composition non-uniformity is infrared transmittance spectroscopy [4, 5].

Prior to testing, the samples were cleaned in organic solvents followed by a Br-methanol etch and a final rinse in deionized water. The room-temperature transmission curves were recorded using a PE983 infrared spectrophotometer with a fine resolution of transmittance of more than 10^{-3} . The SIMS depth profiles were measured at Fudan University using O_2^+ primary-ion bombardment. The erosion rate for $\text{Hg}_{1-x}\text{Cd}_x\text{Te}$ is about 0.8 $\mu\text{m min}^{-1}$.

Figure 1 shows typical fits to measured room-temperature transmission for $\text{Hg}_{1-x}\text{Cd}_x\text{Te}$ epilayers fabricated by three different growth techniques. The full circles are experimental data. The solid curves are calculated from equations (1)–(7), while the dotted curves in figures 1(b) and (c) are derived from equations (1)–(8). The interference fringes in figures 1(a) and 1(c) will make the parameter H difficult to identify, but it does not affect the composition profile. The small deviations in figures 1(b) and 1(c) between the calculated result (solid curve) and experimental data in the absorption edge are caused by the transverse composition non-uniformity [5, 7]. We measured the 300 K infrared transmittance spectra at different spots on the wafers and find that for MBE samples, all curves coincide with each other but, for LPE and MOCVD samples, the curves have some divergences at different measuring points. For this reason, the transverse composition for the MBE sample is constant, but those for the measured LPE and MOCVD samples vary. The fairly good agreement between the calculated curves (dotted curves) in figures 1(b) and 1(c) and experimental data implies that equation (8) is suitable for describing the spatial composition distribution containing both the longitudinal and the transverse non-uniformities.

Figures 2(a), 2(b) and 2(c) are the composition profiles corresponding to figures 1(a), 1(b) and 1(c), respectively. The longitudinal composition profile in figure 2(a) is derived from equations (1)–(7), with the determined fitting parameters x_s , s and dz . The spatial compositional distributions in figures 2(b) and 2(c) are deduced from equations (1)–(8) by further considering the composition deviation in the epilayer plane. σ values in equation (8) are 0.0015 and 0.005 for LPE and MOCVD samples, respectively. For comparison, the SIMS depth profiles of Hg in figures 3(a) and 3(b) and the surface Te concentrations measured by the x-ray microprobe method are also presented for the MBE and LPE samples.

Figures 2(a) and 3(a) are compositional profiles for the MBE layer. From figure 3(a), the position of the $\text{Hg}_{1-x}\text{Cd}_x\text{Te}$ –CdTe interface and CdTe buffer layer can be ascertained from the Te profile. The epilayer surface affects the transmission strongly, and its Cd concentration of 0.239 derived from the equation (7) agrees well with the value of 0.2378 obtained from x-ray microprobe measurement. The concentration changes slightly from the surface to the interface and sharply in the interface region in both figure 2(a) and figure 3(a). The epilayer–substrate interfacial region influences the transmission weakly; so its composition distribution in the region determined from 300 K transmission is less accurate. For example, the interface region in figure 2(a) is narrower than that in figure 3(a).

Figures 2(b) and 3(b) are composition profiles for the LPE layer. The secondary-ion counts become undulating at the end of the epilayer because the number of mercury ions detected is small. The calculated Cd mole fraction at the surface is in the range of 0.1845–0.1875, which agrees well with the measured result, 0.1854. At the same time, the derived

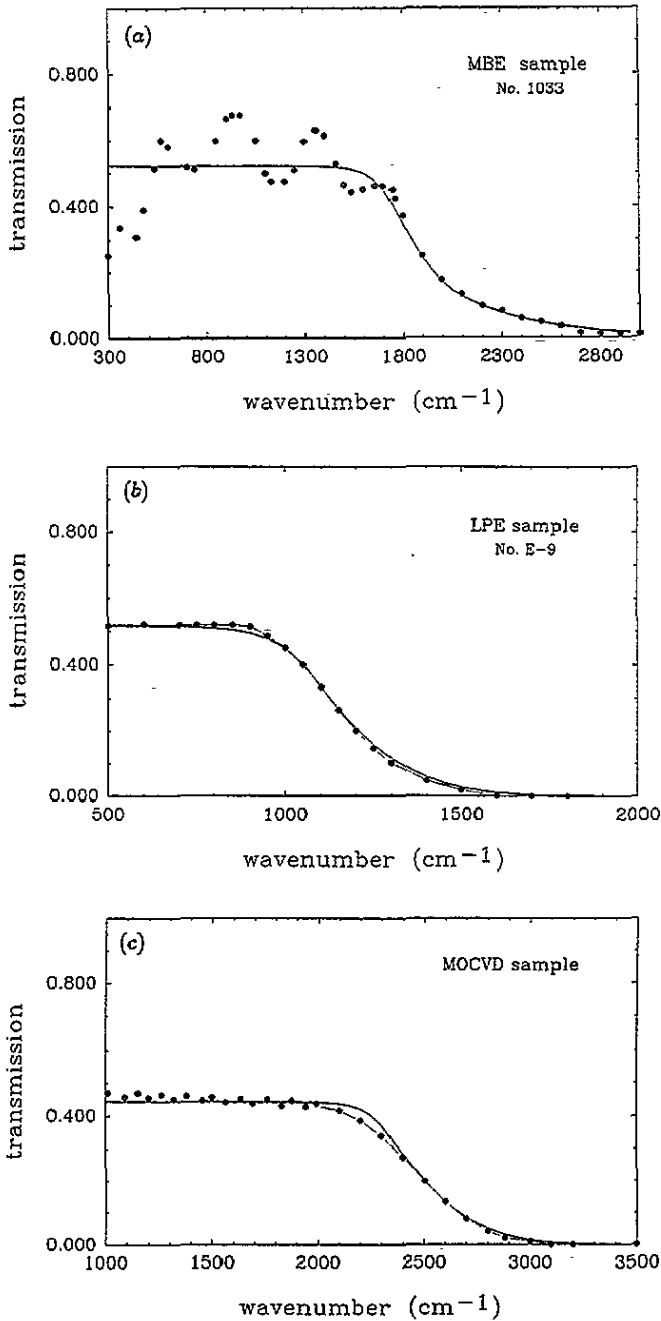


Figure 1. Room-temperature infrared transmission of $\text{Hg}_{1-x}\text{Cd}_x\text{Te}$ films fabricated by (a) MBE, (b) LPE and (c) MOCVD: ●, measured data; —, calculated from equations (1)–(7); ·····, derived from equations (1)–(8).

composition curve in figure 2(b) fits the SIMS depth profile qualitatively. The non-uniformity of transverse composition and the uncertainty of the epilayer thickness due to the rough surface are the main sources of deviations.

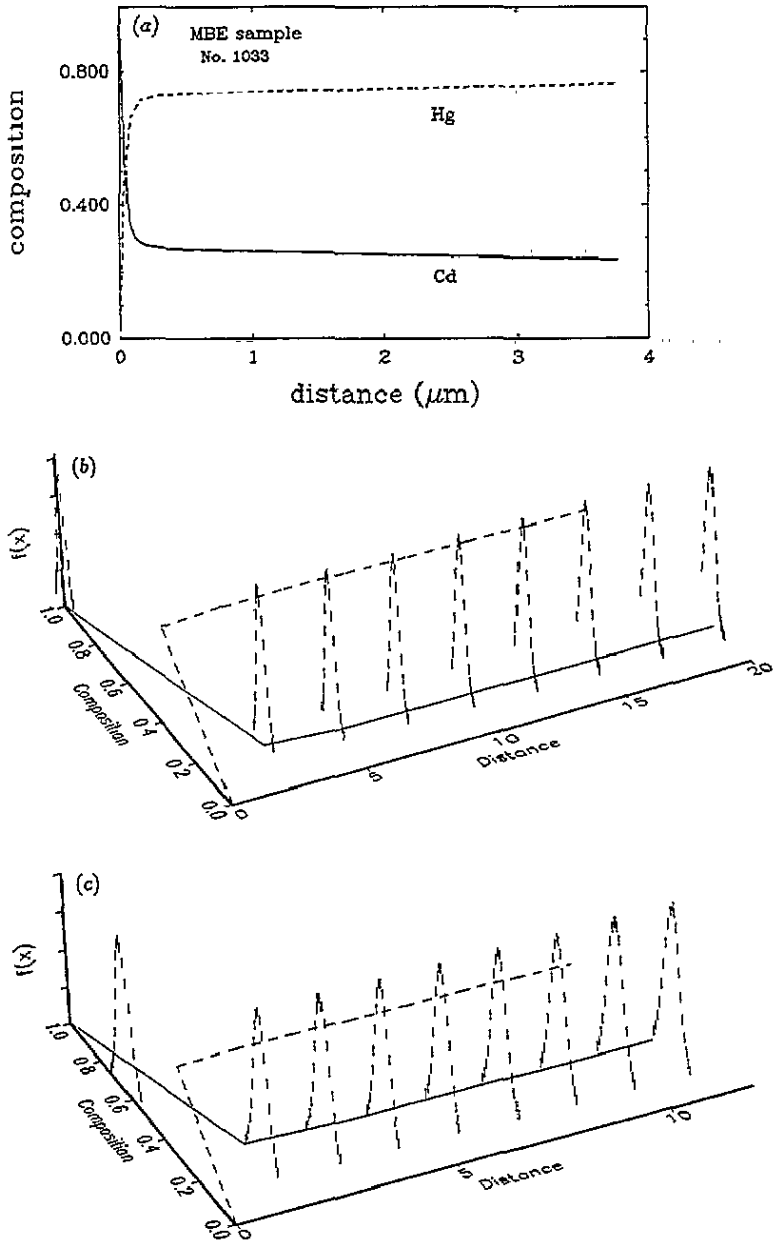


Figure 2. (a) Longitudinal composition profiles of MBE $\text{Hg}_{1-x}\text{Cd}_x\text{Te}$ film, (b) spatial composition distribution of LPE layer with $\sigma = 0.0015$ and (c) spatial composition distribution of MOCVD layer with $\sigma = 0.005$: —, Cd concentration profile; ----, Hg mole fraction curves.

4. Conclusion

In this paper we have presented a method for determining the compositional depth non-uniformity of $\text{Hg}_{1-x}\text{Cd}_x\text{Te}$ films fabricated by different growth techniques. The results show that our empirical rules for the intrinsic absorption coefficient and refractive index of

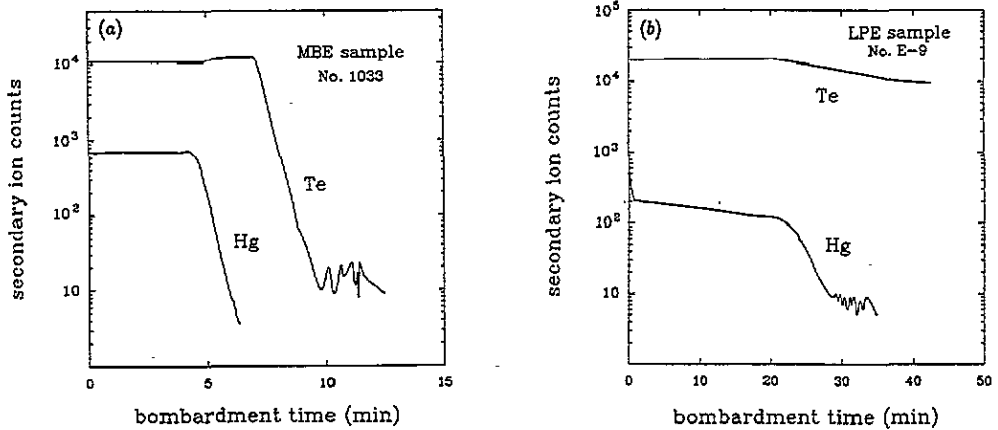


Figure 3. SIMS depth profiles of $Hg_{1-x}Cd_xTe$ films for (a) a MBE sample and (b) a LPE sample.

$Hg_{1-x}Cd_xTe$ in Hougen's model are valid for thin-film materials. A more exact explanation of experimental results should consider the transverse composition non-uniformity.

Acknowledgments

The authors would like to thank Professor S X Yuan, Professor Z Z Yu, Mr X Q Chen and Ms J Y Cao for supplying samples. Thanks are also due to Ms H M Ji for performing the transmission measurements and Dr Q H Du for valuable discussions.

References

- [1] Edwall D D, Gertner E R and Tennant W E 1984 *J. Appl. Phys.* **55** 1453
- [2] Bubulac L O, Edwall D D and Cheung J T 1992 *J. Vac. Sci. Technol.* **B 10** 1633
- [3] Price S L and Boyd P R 1993 *Semicond. Sci. Technol.* **8** 842
- [4] Chu J H, Shiqiu X, Huamei J, Zhang Weizu, Cheng Shiwei and Jiang Rongjin 1985 *Chin. J. Infrared Res.* **4** 255
- [5] Chu J H, Miao Jingwei, Shi Qiao, Liu Kun and Ji Huamei 1992 *J. Infrared Millim. Waves* **11** 411
- [6] Hougen C A 1989 *J. Appl. Phys.* **66** 3763
- [7] Gopal V, Ashokan R and Dhar V 1992 *Infrared Phys.* **33** 39
- [8] Chu J H, Mi Z Y and Tang D Y 1992 *J. Appl. Phys.* **71** 3955
- [9] Chu J H, Li B, Liu Kun and Tang D Y 1994 *J. Appl. Phys.* **75** 1234
- [10] Liu Kun, Chu J H and Tang T Y 1994 *J. Appl. Phys.* **75** 4176
- [11] Liu Kun, Chu J H, Li B and Tang D Y 1994 *Appl. Phys. Lett.* **64** 2818